Plant Physiol. (1977) 60, 127-139

Diffusion Mechanism for Phyllotaxis

THEORETICAL PHYSICO-CHEMICAL AND COMPUTER STUDY

Received for publication August 19, 1976 and in revised form February 22, 1977

ARTHUR H. VEEN AND ARISTID LINDENMAYER
Theoretical Biology Group, University of Utrecht, Padualaan 8, Utrecht, The Netherlands

ABSTRACT

The mechanism for leaf position determination by the diffusion of an inhibitor has been studied in relation to the geometry of leaf positions. A computer model has been constructed for the inhibitor-diffusion process on a cellular cylindrical surface. The behavior of the model has been analyzed mathematically. The main results are: (*a*) that our model generates most of the phyllotactic patterns observed in nature; and (*b*) that restraints have been found for permissible values of diffusion rates and decay rates of the hypothetical inhibitor.

Phyllotaxis, the study of leaf arrangements on growing shoot apices, is a field of longstanding interest and with a very extensive literature. Unfortunately, its literature falls into two rather distinct areas: the geometric description of phyllotactic patterns found in nature, or constructed theoretically, and the attempts to find physiological and cytological mechanisms responsible for initiation of leaf primordia. It seems to have been entirely possible to investigate one of these areas without paying any attention to the other. As far as the physiological mechanisms go, over many years many hypotheses have been put forward, such as Schwendener's mechanical pressure hypothesis (1, 18), the inhibitor-diffusion hypothesis of Schoute (16) and Richards (15), the first available space theory of Snow and Snow (19), the foliar helix hypothesis of Plantefol (14) and a nutrient depletion hypothesis. In our opinion, two of the above mechanisms (the inhibitor-diffusion and the first available space hypotheses) are indistinguishable as far as their consequences are concerned. Recently Williams (23) has expressed a preference for a "mechanical-chemical field theory," meaning a combination of mechanical forces (like pressure) and physico-chemical processes (like diffusion) bringing about the correct placing of the leaf primordia.

Our purpose is to show how one can formulate one of the above hypotheses in such a precise way that one can bridge the gap between the physiological mechanisms and the geometric descriptions. We have constructed a computer model for phyllotaxis based on the inhibitor-diffusion hypothesis which is on the one hand physico-chemically realistic and on the other hand produces results that are comparable to anatomical-morphological observations.

From the mathematical point of view, the problem is to obtain concentration values on a growing apical surface with varying numbers of point sources of inhibitor. This problem is unsolvable by mathematical analysis. A reasonable approximation can be achieved by dividing the surface into subunits and computing the concentrations in each subunit iteratively. For the sake of computer implementation a growing cylindrical surface was chosen. For many plants the portion of the apex on which primordia are generated can be reasonably approximated by a cylinder. Many other plants, however, have flattened apices, and for the phyllotaxis of these cases a planar model has been constructed, the publication of which is in preparation (*cf.* 22).

Our paper presents two main results. First, our model generates all packed circles patterns. Among workers in this field there is a general agreement that this class of patterns (defined in the next section) covers most phyllotactic arrangements found in nature. Second, restraints have been found which lead to intervals of permissible values for diffusion rates and decay rates of the hypothetical inhibitor. A formal relationship has been found between geometric and physiological parameters of the model, and insight has been gained concerning the frequent connection of Fibonacci numbers and phyllotactic patterns.

GEOMETRY OF PHYLLOTAXIS

For the purpose of this discussion, we adopt the hypothesis that by good enough approximation, the area in the plant where leaf initiation takes place is a cylinder and that the leaf centers on this surface form a *regular point system*. These geometrical constructs were studied in elaborate detail by Van Iterson (21) while shorter versions can be found in Erickson (ref. 3; and "Mathematics of phyllotaxis: a reappraisal" [manuscript]) and Veen (22). Here we will give only a summary of the mathematical definitions and results as far as needed for the discussion of our model. They are characterized by the parameters α, the *divergence angle* and h, the *horizontal displacement* such that between every two consecutive leaves the horizontal and vertical separation is constant and equal to α and h. This means that the shortest line connecting all consecutive leaves forms a helix which is called the *generative helix*. If we choose an arbitrary leaf as leaf 0, we thus have a natural numbering of the leaves. In Figure 1a a regular point system is displayed while in 1b we see the unrolled surface of the same cylinder. Here the generative helix is not shown but three other helices are drawn. On one of these, going through leaves 0 and 3, the numbers of two consecutive leaves differ by 3. This is called a 3-parastichy. Also one of the 5- and one of the 8-parastichies are drawn. In general there are m parallel m-parastichies covering all leaves. Again the spacing along an m-parastichy is uniform and is called d_m. For each system there is an m such that d_m is minimal: leaf 0 and m are nearest neighbors. A special class of regular point systems are those for which there are two different integers m and n such that $d_m = d_n$. So leaf 0 has as nearest neighbors $-m$, $-n$, m, and n and equal distance d to all of them. If we drew around all leaves circles with diameter d as in Figure 2, then all circles would touch four others and none would overlap, for which reasons these are called *packed circles systems*, or if $d = d_m = d_n$ and $m < n$ (m,n)-*systems*. Figure 2b shows a (2,3)-system. We shall call the integers m,n-contact numbers. These packed circles systems and the parameter d are of special interest for our model as we will clarify later. There is an (m,n)-system for every m and n without common divisor. The following relation holds between α, d, m, and n.

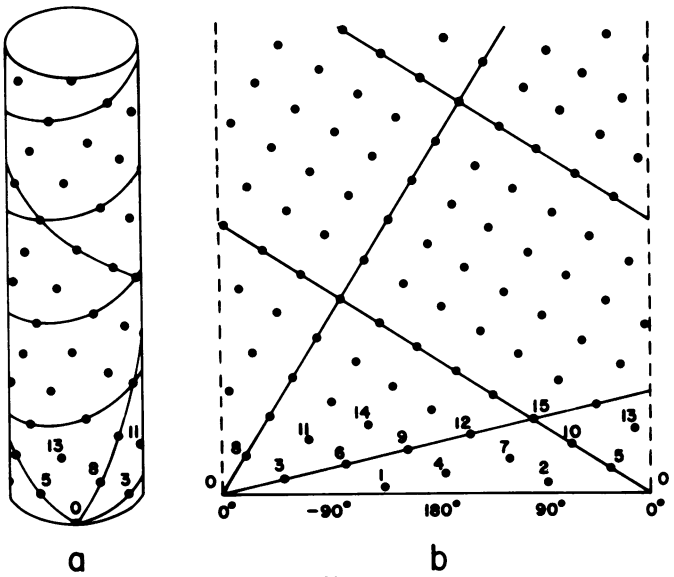

FIG. 1. a: Regular point system on a cylinder surface; b: on the unrolled surface the 3-, 5-, and 8-parastichies through point 0 are shown. Reproduced from reference 3.

$$\alpha = s_\Delta \frac{(n^2 - m^2)d^2 + 4\pi^2}{4mn\pi} + \frac{\Delta_m}{m} 2\pi \qquad (1)$$

Here $s_\Delta = \pm 1$ and Δ_m is an integer, which are directly related to m and n by formulas which we will not give here.

We see that for every pair (m, n) α is a quadratic function of d, so that if we plot α *versus* d for all valid combinations of m and n we get a collection of parabolas (Fig. 3). However, there will not be an (m,n)-system for every α. In Figure 2b α is 138.5° and d is 1.74. If we decrease d gradually and keep adjusting α according to formula 1 we get to the point in Figure 2c where we have $d_2 = d_3 = d_5$. This is called a (2,3,5)-system, a *triple point,* or a *hexagonally packed system.* If we continue to decrease d and stay within formula 1 the circles along the 5-parastichy will overlap so $d_2 = d_3 > d_5$. So the (2,3,5)-point is a limiting point of the (2,3)-system as is the (1,2,3)-system on the other side (Fig. 2a). In general, the validity of formula 1 for every (m,n)-system is limited by the two triple points $(n\text{-}m, m, n)$ and $(m, n, m + n)$.

The relation between these numbers n-m, m, n, $m + n$ is identical to that between any four consecutive members of a well known mathematical series called the *summation series* in which every member is the sum of the previous two. The series starting with 0 and 1 is the famous Fibonacci series.

0, 1, 1, 2, 3, 5, 8, 13, 21, 34, 55, 89, ...

These numbers are frequently found in connection with phyllotaxis, a fact which has been puzzling to many workers and mystifying to others. We return to this problem later. We can already see in Figure 3 that starting at (0, 1, 1) descending down the branches and taking the steepest branch at every triple point, we obtain pairs or triples of consecutive Fibonacci numbers for the nearest neighbor numbers we encounter.

The patterns discussed so far are all simple helical systems, *i.e.* there is only one generative helix. Many plants, however, have two leaves at the same level on the stem. Here we can find two generative equidistant helices and when we cut the surface into two equal parts we obtain two identical helical systems. The double pattern is called bijugate and if it is a packed circles system the notation is $2(m, n)$. Similarly we have trijugate and in general J-jugate patterns with the notation $J(m, n)$. J is called the jugacity.

DESCRIPTION OF THE MODEL

Our model is based on the inhibitor-diffusion hypothesis of the generation of leaf primordia as expressed in the following biological assumptions.

1. In many plants the part of the apex where leaf initiation takes place can be approximated by a cylinder. Its cells are of approximately the same size and are arranged in a regular fashion.
2. The phyllotaxis is regulated by a compound, called the inhibitor, which is diluted or broken down at a constant rate and which diffuses isotropically over the surface in such a manner that the concentration within a cell is uniform and concentration gradients are established mainly across the cell walls.
3. The center of each leaf produces this inhibitor.
4. The center of the apex represented by the upper circle of the cylinder also produces this inhibitor.

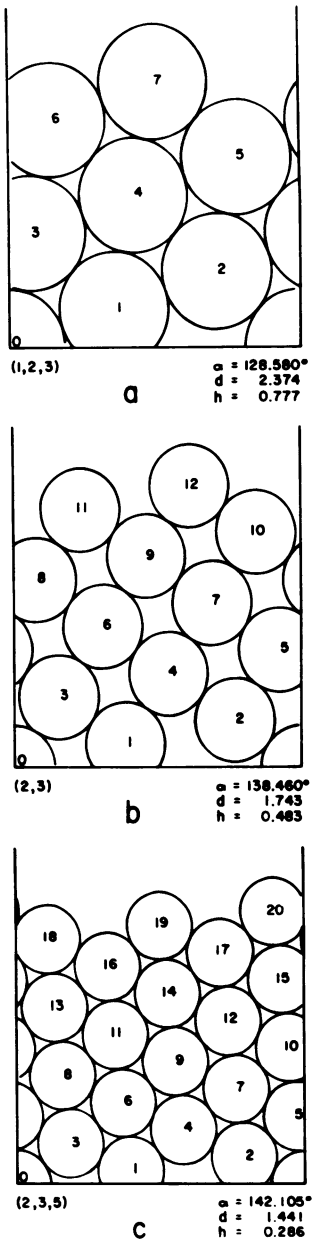

FIG. 2. Packed circles pattern on an unrolled cylinder surface. α is divergence angle, d is diameter of the circles, h is vertical displacement.

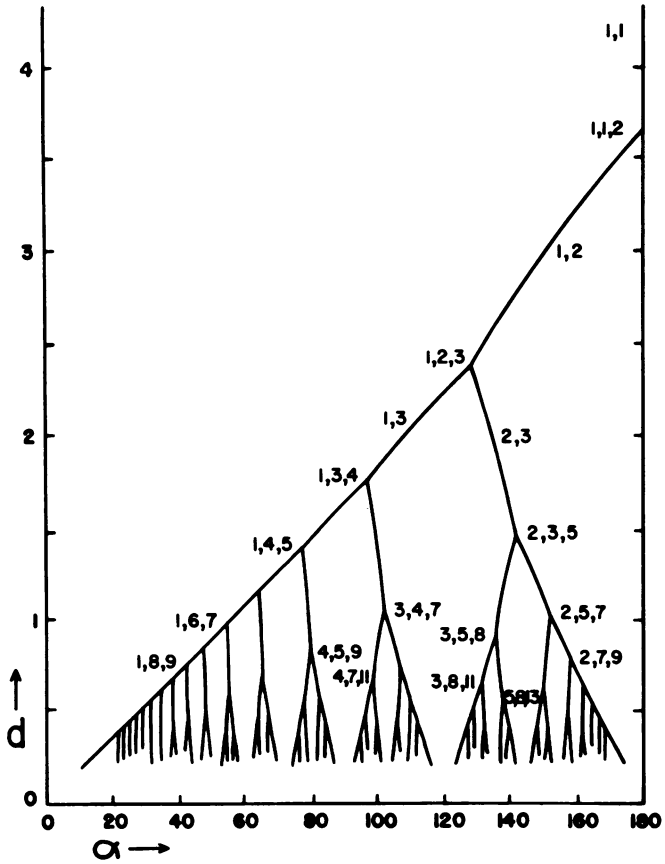

FIG. 3. Relation between diameter and divergence angle for packed circles patterns on cylinder surfaces. Nearest neighbor numbers are shown for the most important branches and triple points.

5. Each cell in which the concentration of the inhibitor drops below a certain threshold becomes a leaf center.

6. Cell division and growth take place mainly at the top of the cylinder, that is, above the initiation area.

These assumptions about the processes in plants find their equivalents in the following features of the model.

1. The geometric basis of the model is an array of cells arranged on a square grid with the left and right sides of the network connected to obtain the topological equivalent of a cylinder surface.

2. Diffusion is simulated in time steps. Each cell is assigned an initial concentration of inhibitor. At every step the next concentration of each cell is derived from its old concentration and that of its eight nearest neighbors according to the decay-diffusion formula.

3. Certain cells are in a special state, called "leaf center" or "leaf," in which the cell maintains a constant concentration L of the inhibitor.

4. The top ring of cells maintains a constant concentration A of the inhibitor.

5. Each cell in which the concentration of the inhibitor drops below a certain threshold T turns into a leaf center.

6. Every G time steps a new row of cells with concentration A is added to the top of the cylinder freeing the previous top row to take part in the decay-diffusion process.

Only under very special conditions can an accurate prediction of the behavior of this model be made. For all nontrivial cases an actual simulation of the model has to be performed. We incorporated this model in a computer program to carry out these simulations.

The assumptions concerning the production and diffusion of an inhibitor are formally related to another set of assumptions concerning the consumption and diffusion of an inducer or a nutrient. It is our feeling that the results of these latter assumptions would closely parallel those of the inhibitor-diffusion hypothesis, but we have not pursued this line of thought.

We assume the inhibitor to diffuse isotropically (that is with no preferred direction) according to Fick's law in two dimensions and to decay proportionally to the concentration. The rate of concentration change $\frac{\partial c}{\partial t}$ at point (x, y) is

$$\frac{\partial c}{\partial t} = \lambda^* \left(\frac{\partial^2 c}{\partial x^2} + \frac{\partial^2 c}{\partial y^2}\right) - D^* c \qquad (2)$$

in which λ^* is the diffusion constant and D^* is the decay constant. This represents diffusion in a continuous medium. In our cellular model we deal in fact with two transport processes: the transport within the cell which is extremely fast due to streaming, and the diffusion through the cell wall or membrane. We assume that the time needed by the internal diffusion is insignificant compared to that of the intercellular diffusion and that the significant diffusion gradients are established across the cell walls. If we substitute the concentration gradients along the two dimensions

$$g_x = \frac{\partial c}{\partial x}$$

and

$$g_y = \frac{\partial c}{\partial y}$$

in formula 2 we get

$$\frac{\partial c}{\partial t} = \lambda^* \left(\frac{\partial g_x}{\partial x} + \frac{\partial g_y}{\partial y}\right) - D^* c$$

Since we assume concentration throughout a cell to be equal, this is equivalent to the finite difference formula

$$\frac{\partial c}{\partial t} = \frac{\lambda^*}{\Delta l}([g_{x_1} - g_{x_2}] + [g_{y_1} - g_{y_2}]) - D^* c \qquad (3)$$

where g_{x_1} and g_{x_2} are the gradients at the left and the right sides of the cell, and g_{y_1} and g_{y_2} at the bottom and top, while Δl denotes the diameter of the cell. If we have a cell with concentration c_0 surrounded by eight neighboring cells with concentrations c_i as in Figure 4, we have to express the gradients as a function of

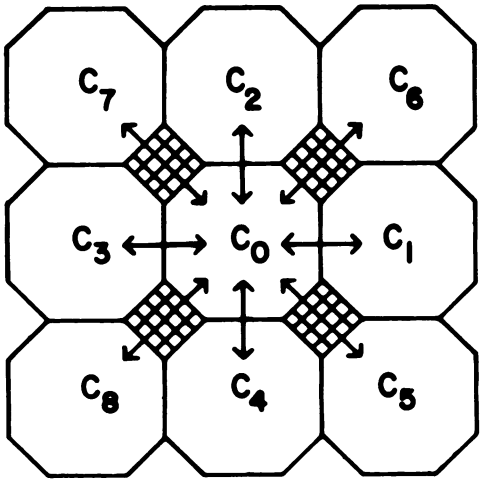

FIG. 4. Patterns of neighboring cells determining the diffusion formula, where each cell interacts directly with eight neighbors as used in our model.

the concentrations. Let the corner cells take part q in the establishment of the gradient. We get a formula

$$g_{x_1} = ([1 - 2q][c_3 - c_0] + q[c_6 - c_0] + q[c_7 - c_0])/\Delta l$$

and similar ones for g_{x_2}, g_{y_1}, and g_{y_2}. These substituted in formula 3 lead to

$$\frac{\partial c_0}{\partial t} = \frac{\lambda^*}{(\Delta l)^2}\left(\left[1 - 2q\right]\sum_{i=1}^{4} c_i + 2q\sum_{j=5}^{8} c_j - 4c_0\right) - D^* c_0 \quad (4)$$

For efficiency and other programming reasons we chose $q = 1/4$, leading to

$$\frac{\partial c_0}{\partial t} = \frac{\lambda^*}{2(\Delta l)^2}\left(\sum_{i=1}^{8} c_i - 8c_0\right) - D^* c_0 \quad (5)$$

Digitalizing the time scale with time unit Δt, (5) becomes

$$\Delta c_0 = \lambda^* \frac{\Delta t}{2(\Delta l)^2}\left(\sum_{i=0}^{8} c_i - 9c_0\right) - D^* c_0 \Delta t \quad (6)$$

Substituting the diffusion constant in terms of our time and distance units

$$\lambda = \lambda^* \frac{\Delta t}{2(\Delta l)^2} \quad (7)$$

and the decay constant

$$D = D^* \Delta t \quad (8)$$

we arrive at the formula actually used in the program

$$c_0 = c_0 + \Delta c_0 = \lambda \sum_{i=0}^{8} c_i + (1 - 9\lambda - D)c_0 \quad (9)$$

We can see from this formula that if λ is greater than $1/9$ or D greater than 1 the new value of c_0 will be inversely dependent on its old value. This might very well lead to unrealistic oscillations. For this reason we set upper limits on λ and D, which are merely reflections of an upper limit on Δt. This indicates that the digitalization of the process cannot be arbitrarily coarse.

AUTOMATA-THEORETICAL MODELS FOR MULTICELLULAR DEVELOPMENT

Computer-oriented models have been proposed by one of us (7–9) to describe the development of multicellular organisms. In these models, cells are considered to be finite automata, with finitely many states, inputs, and outputs. The cells of a filamentous organism are represented by a linear array of automata, in which each cell can receive inputs from its two neighbors and contribute outputs to them. The next state of a given cell is computed in discrete time steps on the basis of its previous state and the inputs it receives. New cells may be added to the array anywhere (corresponding to cell divisions) and cells may disappear from them (by cell death). An extensive biological and mathematical literature is now available on these models (6, 10). They have been called $0L$-, $1L$- or $2L$-systems depending on whether the automata receive no input, input from one direction, or from two directions in the one-dimensional array. An extension of these models to multidimensional arrays has recently been accomplished on the basis of graphs.

Concerning the present problem, two-dimensional cellular arrays have already been described above (Fig. 4); these can be considered as examples of graph L-systems in which each cell is placed on a cylindrical grid and has always either four or eight neighbors. The inputs to the cells are the concentrations of the morphogen in the neighboring cells. The new morphogen concentration for a given cell is computed on the basis of these inputs and the state of the cell itself (its own concentration) with the help of formula 9. The same formula is used for all of the cells. The only exceptions are those cells in which the morphogen concentration has fallen below the threshold; these cells have become primordia and are assigned constant concentration values. Addition of new cells can only take place by adding new rows of cells at the top of the array. To the cells in the top and bottom rows environmental inputs have to be provided, which is achieved by adding two rows of cells at the top and bottom which are kept at constant values. The computations are performed simultaneously on all of the cells of the array, thus satisfying all of the conditions of a deterministic, eight-neighbor graph *L-system*.

COMPUTER PROGRAM

The cylindrical model has been incorporated in the program BLOCKO written in ALGOL 60. It can be controlled interactively from a terminal so that its computation can be interrupted at any time step to change parameters or define new leaves. For the starting configuration we choose: the circumference of the cylinder in number of columns of cells w; the initial height in number of rows of cells R; the top row or apex concentration A; the initial concentration B of all other cells.

At this point as well as later we can define certain cells as leaves, that is assign them a constant concentration. In this way an initial distribution of leaves can be defined and the first question we studied was if it was possible to choose the parameters such that this initial distribution will be reproduced by the model.

After we have set the other parameters and started the computation, the program applies the decay-diffusion formula 9 independently to all cells, and it chooses for the c_i values entering this formula always the concentrations before the current time step. At the end of every time step all cells that have dropped under the threshold T are assigned the constant leaf value L or alternatively under the "erase" option, of a connected group of those cells only the one with minimum concentration is made into a leaf.

Growth is incorporated by adding a new row of cells every G time steps. This corresponds to a real growth rate of

$$g^* = \frac{\Delta l}{G\Delta t} \quad (10)$$

from which we see that G is the reciprocal growth rate.

In summary, the crucial parameters of the model are: decay constant (D), diffusion constant (λ), leaf cell concentration (L), threshold concentration (T), reciprocal growth rate (G), apex or top row concentration (A), width of the array or number of cells on the circumference of the cylinder (w), initial concentration (B), initial number of rows (R), positions and time steps of insertion of initial leaves. The parameters D, λ, L, T, G, and A can be changed dynamically.

COMPUTER-GENERATED PHYLLOTACTIC PATTERNS

Detailed Demonstration. To illustrate the performance of the model we discuss a demonstration in detail. At the start we set the parameters as in Figure 5 and insert a leaf in column 1 row 3. The first printout after one complete computation can be seen in Figure 5a. This is the symbolic representation of the state of the model. The concentration of a cell is rounded to its nearest integer and converted to a symbol according to Table I.

For higher values the integer modulo 80 is taken and an additional bar is printed through the symbol. Leaf cells are marked by solid squares. The numbers on the left are the row numbers.

It can be seen that the top and bottom rows stay at concentration 5. Across most cell walls there is no concentration gradient

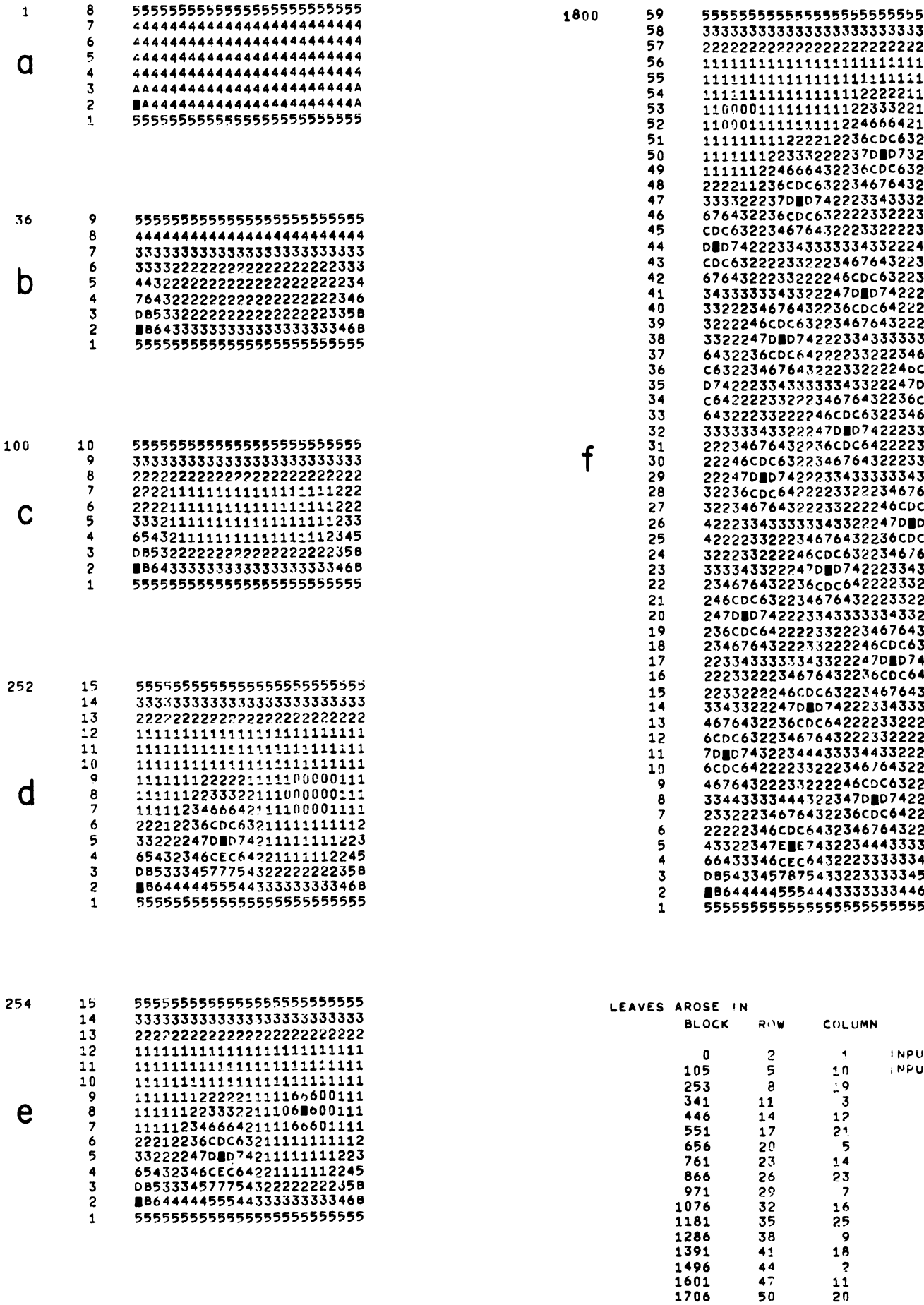

FIG. 5. Detailed demonstration of the simulation of a (2,3)-pattern with $\alpha = 129.6°$ and $d = 2.318$. The parameters were set at: $D = 0.1$, $\lambda = 0.1111$, $L = 50$, $T = 0.4$, $G = 35$, $B = 5$, $A = 5$, $R = 8$, $w = 25$. The first two leaves were put in at predetermined locations (row 2 column 1; row 5 column 10) at time steps 0 and 105. The third leaf arose at step 253. The last array, at step 1,800, shows 17 leaves.

Table I

Symbolic representation of concentrations in the computer printouts

```
0123456789ABCDEFGHIJKLMNOPQRSTUVWXYZ:ABC
0         10        20        30
DEFGHIJKLMNOPQRSTUVWXYZ:+-*/; = <(>[]){}vA
40        50        60        70        80
```

so these cells get a concentration $(1 - D)\ B = 4.5$. Only the neighbors of the leaf cell experience the influence of its high concentration. The leaf cell stays at concentration 50.

After 35 computations the first growth step takes place. Row 9 is added and row 8 can now freely engage in the diffusion-decay process (Fig. 5b). After 100 time steps it is clear that the lowest concentrations can be found on the middle rows as far away as possible from the leaf in column 1 because the concentration distribution at this point is completely mirror symmetrical around it.

Since we want to demonstrate a nonsymmetrical pattern, we have to insert at least one more leaf. We place this second leaf three rows above and nine columns to the right of the first one.

The printout after time step 252 reveals that by this time the distance between the youngest leaf and the apex is large enough to allow some cells to drop to a very low concentration. All Os indicate concentration values below 0.5. In Snow's terminology, there is enough space available; that is, there are cells far enough removed from both the apex and the other leaves to drop to threshold value. In time step 253 the first generated leaf appears at row 8 column 19. The next leaf comes in at row 11 column 3. We let the program run through 1,800 time steps and the final state can be seen in Figure 5f.

The list of the birth dates and positions of all of the leaves reveals that the displacement between the two inserted leaves has been reproduced so that between two successive leaves there is always a horizontal distance of nine cells ($u = 9$) and a vertical distance of three rows ($v = 3$). Here we have a cylinder with a circumference of 25. To compare this pattern to those on the cylinders in the geometry section, which have a circumference of 2π we need to normalize our distances, that is multiply by $2\pi/25$. Then we see that we actually have generated a simple helical pattern with a divergence angle $\alpha = 2\pi\ (u/w) = 2\pi\ (9/25) = 2.26 = 129.6°$ and a normalized vertical displacement with $h = 2\pi\ (v/w) = 2\pi\ (3/25) = 0.755$. The normalized distance between the first and second leaves is

$$d_1 = \sqrt{v^2 + u^2}\,\frac{2\pi}{w} = \sqrt{3^2 + 9^2}\,\frac{2\pi}{25} = 2.378$$

Similarly, we get $d_2 = d_3 = 2.318$. So we have a packed circles pattern with $\alpha = 129.6°$ and $d = 2.318$ very close to the (1,2,3)-triple point in Figure 2a.

The special significance of packed circles patterns can now be clarified. Each leaf cell produces an inhibitor-filled field centered around itself. Because of the isotropic diffusion this field is basically circular in form; that is, the collection of cells with a particular concentration forms a circle around the leaf cell. Even where the fields of different inhibitor producers join, the resulting field will be basically the addition of the two circles. If we now have a collection of leaf cells positioned on the cylinder as in a packed circles pattern and the parameters of the diffusion process are such that the radius of the inhibited area (that is the collection of cells whose concentration values are kept above threshold by this leaf cell) is equal to the d value of this pattern we will have a situation as illustrated in Figure 6a, where the leaves are positioned as in the computer simulation just described. If we now imagine that because of the growth process the inhibiting influence of the apex moves upward, we see that the first uncovered cell, that is the first cell that will be able to drop under threshold value, will be exactly at the right position to continue the packed circles pattern. It is as if the next leaf appears in the notch left by the three intersecting circles along the 1-, 2-, and 3-parastichies. The notch is the intersecting point of the three circles so it is at equal distances from the three older leaves. This is the same condition that holds for all packed circles patterns. If we consider the same construction with a helical pattern that is not a packed circles pattern as in Figure 6b, we will find the intersecting point M of the two circles along the 2- and 3-parastichies at a different place than that of the next leaf designated L_8.

So we conclude that if we start out with a pattern of leaf cells arranged as in a packed circles pattern and we set the parameters of the model at appropriate values the mechanism will copy the original configuration. This is what we did in this demonstration case. We started out with two leaves in the positions of a (1,2,3)-pattern and we set the parameters to values which we had found to produce the intended results after many trials and failures. In a later section we will describe an analytical formula to determine the right values without having to go through all of the trial runs we made.

Packed Circles Patterns with Integer Positions. The cellularity of the model limits us to certain regular patterns which can be represented on the rectangular grid of the cylinder surface. This is because $\alpha = 2\pi\ (u/w)$, $h = 2\pi\ (v/w)$, and u v, and w are integers (the horizontal and vertical displacements between consecutive leaves and the circumference of the cylinder in numbers of cells). This would present no problems if we would allow arbitrarily large values for w, but both the limited size and speed of computers and the desirability that the number of cells in the apex of the model stays within a reasonable estimate for cell numbers in real apices limit the circumference w to a maximum of about 50. Table II gives all 20 packed circles patterns that can be represented on a cellular cylindrical model with a circumference of 50 cells or less. They are marked on the graph of Figure 7.

Changing the Cell Size. Of course multiples of the values for u, v and w listed in Table II lead to the same pattern. As an example, we simulated the pattern of the previous section on twice as large a scale. This amounts to halving the length unit Δl which has its influence on λ and G according to formulas 7 and 10. Because of the fine scale, the simulation has to be much more accurate and to get meaningful results we had to decrease Δt considerably as we will explain later. Finally, L had to be adjusted to produce the exact pattern.

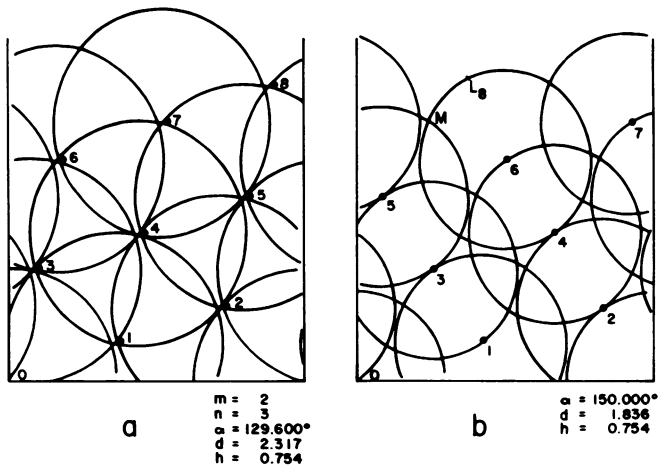

FIG. 6. Construction of intersecting circles on a cylinder surface. a: In a (2,3)-pattern the lowest open space coincides with the next point of the pattern. b: In an arbitrary regular point system the lowest open space (M) does not coincide with the next point of the pattern (L_8).

Table II

Packed circles patterns on a cylinder representable in integer coordinates

The symbols are as follows: w is the number of c cells around the circumference of the cylinder, u and v are horizontal and vertical displacements between consecutive leaves in numbers of cells, m and n are nearest neighbour numbers, α is the divergence angle in degrees, and d is the nearest distances between leaves in cell numbers multiplied by 2π

w	u	v	(m,n)	α	d
5	2	1	(1,2)	144.000	2.8099
10	3	1	(1,3)	108.000	1.9869
13	5	1	(2,3)	138.461	1.7426
15	4	1	(1,4)	96.000	1.7271
15	7	4	(1,2)	168.000	3.3771
17	4	1	(1,4)	84.706	1.5239
24	5	1	(1,5)	75.000	1.3349
25	7	1	(3,4)	100.800	1.2566
25	9	3	(2,3)	129.600	2.3171
26	5	1	(1,5)	69.231	1.2322
29	12	1	(2,5)	148.965	1.1668
34	13	1	(3,5)	137.647	1.0776
35	6	1	(1,6)	61.714	1.0920
37	6	1	(1,6)	58.378	1.0329
39	14	5	(1,2)	129.231	2.3950
40	11	3	(1,3)	99.000	1.7910
41	9	1	(4,5)	79.024	0.9813
48	7	1	(1,7)	52.500	0.9256
50	7	1	(1,7)	50.400	0.8886
50	17	6	(1,3)	122.400	2.2654

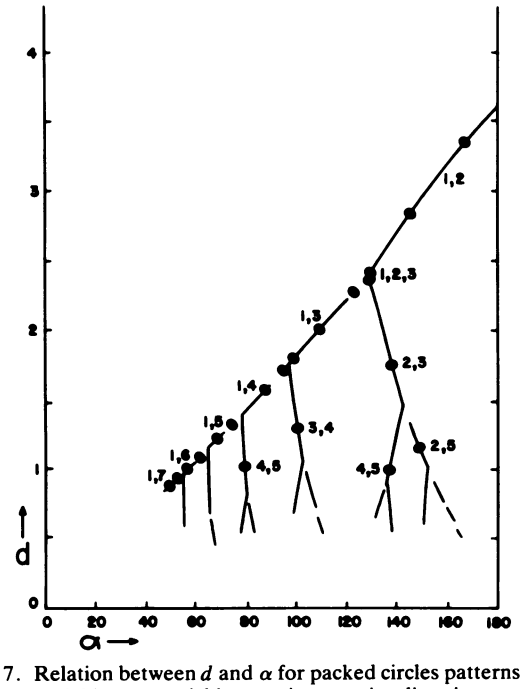

FIG. 7. Relation between d and α for packed circles patterns in which the nearest neighbor parastichies run in opposite directions around the cylinder. The gaps correspond to those patterns in which these parastichies run in the same direction. The patterns of Table II are marked with ●.

The state after 1,200 computations is represented in Figure 8 omitting some symbols so as to emphasize lines of equal concentration. Near the leaves these lines are nearly circles, although here they are distorted into ellipses because of unequal horizontal and vertical spacing between the printer's symbols.

Changing the Time Unit. As our next example let us take the (2,3)-pattern in Table II. Here we have: $w = 26, u = 10, v = 2$, $\alpha = 138.46°, d = 1.74$. This is the system represented in Figure 2b. With three initial leaves at row 2 column 1, row 4 column 11, and row 6 column 21, we get the results of Figure 9a. The first two leaves generated by the system appear at the right positions in rows 8 and 10 but at row 12 an extra leaf appears next to the desired one. The growth of the apex that is responsible for providing enough space for the next leaf takes place in our model in discrete steps. This sudden change has apparently introduced too great a disturbance. The change in concentration in one time step Δc_0 expressed in formula 6 is so large that it overrides any differences in concentrations that might exist between the two cells and it lets them both drop below threshold in one and the same time step. If we can refine the computation process to make Δc_0 in one time step smaller, we might be able to make use of the difference in concentration between the two cells such that in one time step only one of the cells drops under the threshold, turns into a leaf, and effectively inhibits its neighbor in the next time step to turn also into a leaf. We can do this by merely decreasing the size of the time step, Δt. If we want a decrease by a factor of 2, it follows from formulas 7, 8, and 10 that also α and D have to be decreased by a factor of 2 and G increased by the same factor. This corresponds to taking more computer time to obtain a better approximation of the same simulation. This new set of parameters leads to the right helical (2,3)-pattern as can be seen in Figure 9b.

Influence of Growth Rate. We studied the influence of the growth rate on this pattern and found that changes occur only if growth is speeded up to a value such that the reciprocal growth rate G is less than 45. At these high growth rates, double leaves occur again. We concluded that when the growth is sufficiently

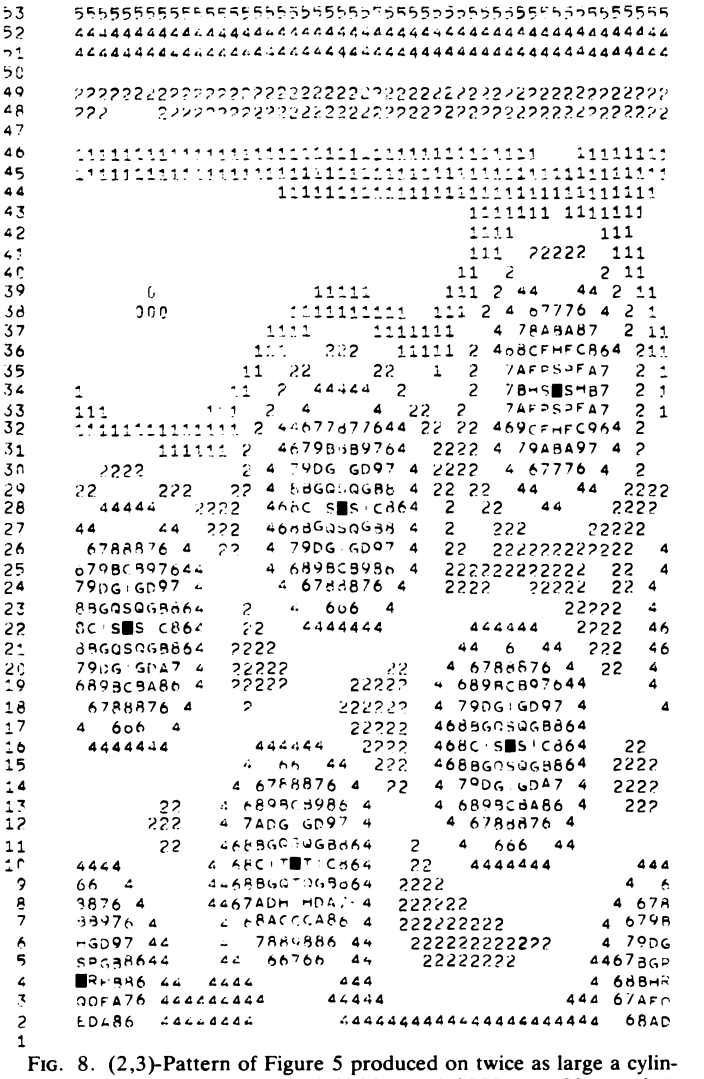

FIG. 8. (2,3)-Pattern of Figure 5 produced on twice as large a cylinder. Parameters were set at $D = 0.0125$, $\lambda = 0.0555$, $L = 75$, $T = 0.4$, $G = 140$, $B = 5$, $A = 5$, $w = 50$. Concentrations falling in specific ranges are represented by blanks to aid visualizing lines of equal concentrations.

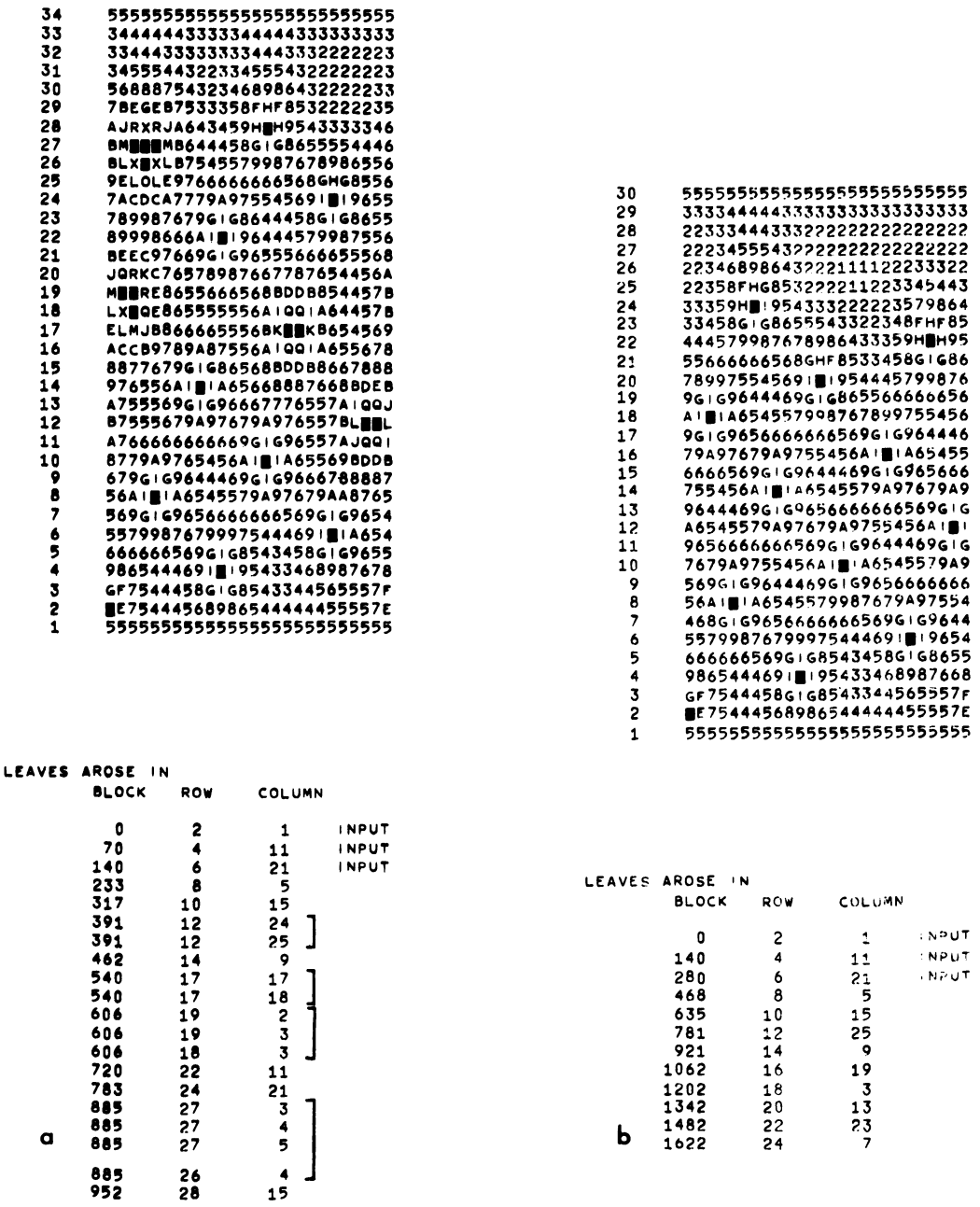

FIG. 9. Production of a (2,3)-pattern with $\alpha = 138.5°$ and $d = 1.74$. a: Parameters set at $D = 0.1$, $\lambda = 0.1111$, $L = 64$, $T = 1.2$, $G = 35$, $B = 5$, $A = 5$, $w = 26$. Double leaves occur, an unsuccessful simulation. b: New parameters obtained by halving Δt: $D = 0.05$, $\lambda = 0.0555$, $L = 64$, $T = 1.2$, $G = 70$, $A = 5$, $B = 5$. Simulation successful.

slow the model comes to a steady-state in between growth steps where the decay and production of inhibitor are in balance and only the growth steps introduce the changes that either lead to another steady-state or to the birth of a new leaf. Consistent with this is that a new leaf usually appears shortly after the influence of a growth step reaches the site of the appearance.

So it is the growth rate that controls the rate of appearance of new leaves while the other parameters control the positions. The analogous situation in a real plant with continuous growth would be that the concentration distribution is in a quasi-steady-state controlled by the λ^*, D^*, L^*, and T^* values while its rate of change is completely dependent on the growth rate. This is consistent with the observation that the phyllotaxis of plants is uneffected by fluctuations in growth rate.

Influence of a Local Disturbance. Figure 10 shows a simulation of the (3,5)-pattern for which $w = 34$, $u = 13$, $v = 1$, $\alpha = 137.65°$, $d = 1.078$. Because in a (3,5)-pattern a leaf is determined by its third and fifth previous leaves, a minimum of five initial leaves is needed to start the pattern. In this simulation the "erase" option has been used (see under "Computer Program"). One could obtain the same pattern without erasing by changing Δt.

In this pattern we also studied how a local disturbance would propagate through the system. We gave the leaf in row 17 three times as high a leaf value as the other leaves. We can see in Figure 10 that this disturbance does not affect the next, the second, and the fourth next leaf positions, but disturbs the position of the third, the fifth, and higher leaves. This is what we would expect from a packed circles (3,5)-pattern where disturbances are only propagated along the contact parastichies.

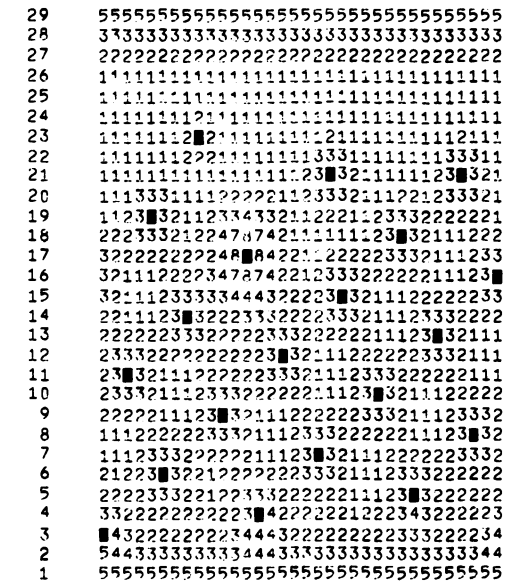

LEAVES AROSE IN BLOCK	ROW	COLUMN	LEAF VALUE	
0	3	1	10	INPUT
140	4	14	10	INPUT
280	5	27	10	INPUT
420	6	6	10	INPUT
560	7	19	10	INPUT
869	8	32	10	
925	9	11	10	
1049	10	24	10	
1192	11	3	10	
1329	12	16	10	
1468	13	29	10	
1607	14	8	10	
1747	15	21	10	
1887	16	34	10	
2026	17	13	30	HIGH LEAF
2167	18	26	10	VALUE
2370	19	5	10	
2574	21	20	10	
2586	21	31	10	
2881	23	9	10	

FIG. 10. Production of (3,5)-pattern with $\alpha = 137.7°$, $d = 1.078$. Parameters set at: $D = 0.025$, $\lambda = 0.0278$, $L = 10$, $T = 0.5$, $G = 70$, $A = 5$, $B = 5$, $w = 34$. Value of the leaf on row 17 column 13 was tripled. Locations of the two nearest leaves after this one have been disturbed.

Trijugate Pattern. Multiple helical systems can be simulated just as easily. Figure 11 shows the simulation of a trijugate helical system that is not exactly a packed circles pattern (since d_2 is less than the other distances) but which is close to the 3(1,1,2)-pattern nevertheless. We have $w = 36$, $u = 6$, $v = 3$, $\alpha = 60°$, $d = 1.044$. The 3(1,1,2)-pattern has $\alpha = 60°$ and $d = 1.21$. In borderline cases like this the model can produce helical patterns which are different from what a packed circles construction would predict. This is especially true for symmetrical cases as here where the initial arrangement of leaves has a perfect symmetry with respect to a rotation of the cylinder over 120°. This symmetry will be retained by the mechanics of the model so that a transition to a real 3(1,2)-pattern that the low value of d calls for is impossible without outside asymmetrical help. It is expected that in plants an asymmetrical configuration would be facilitated by random fluctuations in the concentration distribution. This random influence would induce an equal distribution over left and right handed spirals as is indeed observed in most species.

Unclassified Pattern. A pattern outside the geometric classification of regular point systems but still with a helical periodicity can be seen in Figure 12. From row 10 upward the position of each leaf will be repeated nine rows higher and eight columns to the right. There are six of these separate series of leaves each with a generative helix corresponding to $w = 25$, $u = 8$, and $v = 9$. These helices are indicated in the figure. They run in pairs and if one allows fluctuations in position of one cell unit one could speak of only three generative helices with $u = 4 \pm 1$ and $v = 4.5 \pm 5$.

Transitional Phyllotaxis. An interesting case of changing phyllotaxis can be found in *Bryophyllum tubiflorum*. At least five

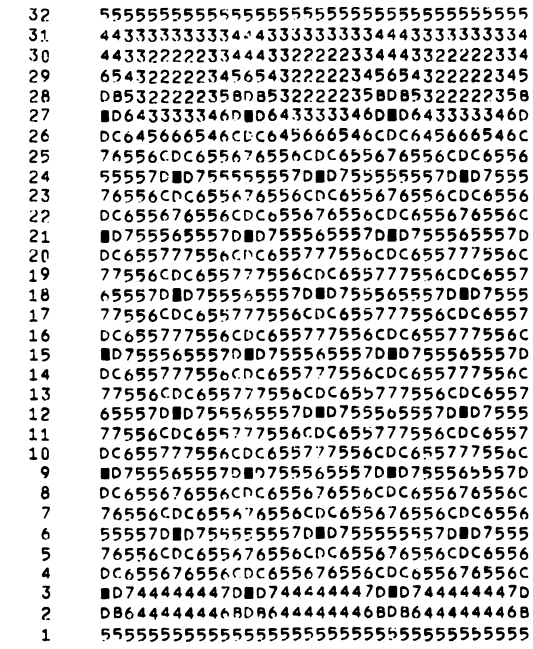

LEAVES AROSE IN BLOCK	ROW	COLUMN	
0	3	1	INPUT
0	3	13	INPUT
0	3	25	INPUT
0	6	7	INPUT
0	6	19	INPUT
0	6	31	INPUT
15	9	1	
15	9	13	
15	9	25	
113	12	7	
113	12	19	
113	12	31	
218	15	1	
218	15	13	
218	15	25	
323	18	7	
323	18	19	
323	18	31	
428	21	1	
428	21	13	
428	21	25	
533	24	7	
533	24	19	
533	24	31	
638	27	1	
638	27	13	
638	27	25	

FIG. 11. Production of a trijugate pattern with $\alpha = 60°$ and $d = 1.044$. Parameters: $D = 0.135$, $\lambda = 0.1111$, $L = 52$, $T = 1.2$, $G = 35$, $A = 5$, $B = 5$, $w = 36$.

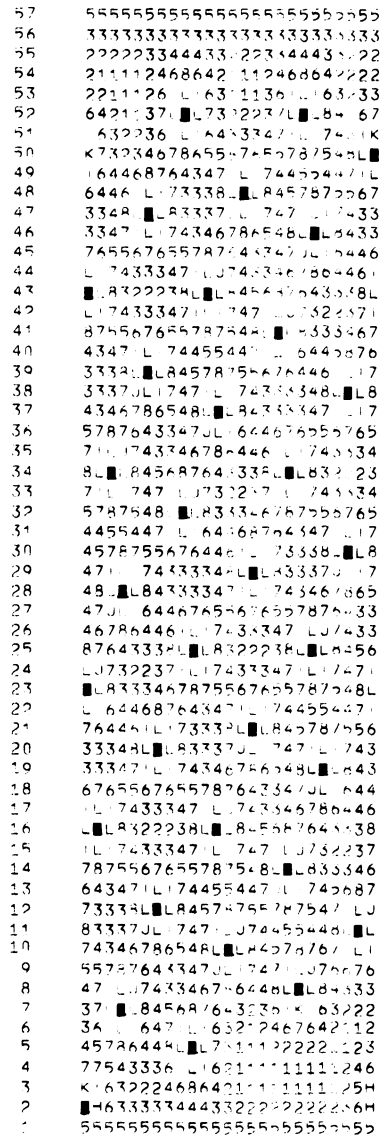

FIG. 12. Production of an unclassified pattern. Parameters: $D = 0.3$, $\lambda = 0.1111$, $L = 122$, $T = 0.4$, $G = 25$, $A = 5$, $B = 5$, $w = 25$.

different phyllotactic patterns can be observed in any full grown plant (4). The change in phyllotaxis from juvenile to adult plants was found to be correlated with a 40% increase in the radius of the free apex (5).

A computer simulation showing this transitional development has been carried out in which the value of L has been gradually decreased from 122 to 12. Decreasing L by a ratio of about 10 corresponds to a decrease in the inhibitory radius r_I of a leaf by a ratio of about 1:3 according to formula 14 (see next section). Since it is the ratio r_I/w that determines the pattern, we can see that a 10-fold decrease in L is equivalent to a 40% increase in the radius of the apex, leaving all other parameters constant. Detailed printouts of this simulation have been published (5).

Phyllotaxis may also change under the influence of chemical agents (11, 13, 17), or as a consequence of juvenile to adult transition. Our proposed mechanism appears to be applicable to these cases.

DISCUSSION

Inhibitory Radius as Function of the Simulation Parameters. To gain more insight into the precise relation between the parameters, D, λ, L, and T, and the inhibiting radius they lead to, a series of 27 simulations was run systematically varying D, L, and T over a wide range and leaving all other parameters and other influences constant. In the 12 most interesting patterns we calculated the smallest distance between leaves r_I. The results are shown in Table III. The patterns are ordered in this table according to the number of leaves produced in 1,600 time steps. This order turns out to be equivalent to the order of increasing contact numbers and decreasing r_I values.

It is to be expected that the smallest distance between leaves, *i.e.* the inhibitory radius r_I, is dependent on the leaf value, the rate of decay, the rate of diffusion, and the threshold value. To find this dependency we shall consider a one-dimensional diffusion mechanism.

Consider an infinitely long one-dimensional tube of which half ($x \leq 0$) is kept at constant concentration L^*. The substance diffuses freely through the tube according to Fick's law with diffusion constant λ^* and decays with decay constant D^*. If we let this process go on for a long time we will get to a steady-state in which

$$\frac{\partial c}{\partial t} = 0$$

Then the general solution for c as a function of x is given by

$$c = K_{\exp}(-x\sqrt{D^*/\lambda^*})$$

where K is a constant (*cf.* ref. 2). At $x = 0$, the concentration has to be equal to L^* so that

$$c = L^*_{\exp}(-x\sqrt{D^*/\lambda^*}) \tag{11}$$

If we think of the source of the constant concentration as situated at a distance s inside of the constant concentration area we get x_I for the distance from the point source to the point at which the concentration is equal to the threshold T^*, and

$$x_I = s + \sqrt{\frac{\lambda^*}{D^*}} \ln \frac{L^*}{T^*}$$

Using the fact that

$$\frac{L^*}{T^*} = \frac{L}{T}$$

and using formulas 11 and 12 we get a formula for the inhibitory distance expressed in cell units Δl:

$$x_I = s + \sqrt{2\frac{\lambda}{D}} \ln \frac{L}{T}$$

For the two-dimensional case where an area around the origin with radius s is kept at constant concentration L^* the solutions for this steady-state are Bessel functions which do not have easy inverses as in formula 11. Nevertheless we can see that the resulting r_I will be dependent on the ratios λ/D and L/T as in

Table III

Series of phyllotactic patterns produced by systematic variations in D, T, and L values

D	T	L	r_I	(m,n)
0.03	0.13	122	22.0	(1,1)
0.03	0.13	45	19.5	(1,1)
0.03	0.40	122	18.8	(1,1)
0.03	0.13	15	15.7	(1,1)
0.03	0.40	45	15.4	(1,1)
0.03	1.20	45	12.0	(1,1)
0.03	0.40	15	11.0	(1,2)
0.10	0.13	45	9.9	(1,2)
0.03	1.20	15	8.5	(2,3)
0.10	0.40	45	8.3	(2,3)
0.30	0.40	45	6.0	2(1,1)
0.30	0.40	15	4.0	3(1,1)

formula 12. We can use the solution for the one-dimensional case (formula 12) to approximate the two-dimensional solution. During a simulation the concentration at the minimum point is the sum of the influences of the two or, in case of a triple contact pattern, three nearest leaves plus some influence of the more remote leaves. This results in the following formula for the inhibitory radius r_I

$$r_I = s + \sqrt{2\frac{\lambda}{D}}\ln\frac{kL}{T}$$

where k is the number of leaves determining the position of the minimum cell having a value between 2 and 3. Making an estimate of 0.6 for the "radius" of a square cell and assuming that $k = e$ we arrive at

$$r_I = 0.6 + \sqrt{2\frac{\lambda}{D}}\left(1 + \ln\frac{L}{T}\right) \quad (13)$$

The values of Table III were plotted and it was found that r_I conforms amazingly well to this formula. A slight adjustment consisting of the substitution of the factor 1.35 for $\sqrt{2} = 1.414$ gives a very good fit to the points in Figure 13 representing some 60 patterns we generated in the course of our research. Because of the cellularity of the model there is always a range in which the patterns are insensitive to small changes in any of the parameters, and this range is approximately the size of a cell.

Most of the patterns of the figure fall within the indicated range, the final formula being

$$r_I = (0.6 \pm 0.6) + 1.35\sqrt{\frac{\lambda}{D}}\left(1 + \ln\frac{L}{T}\right) \quad (14)$$

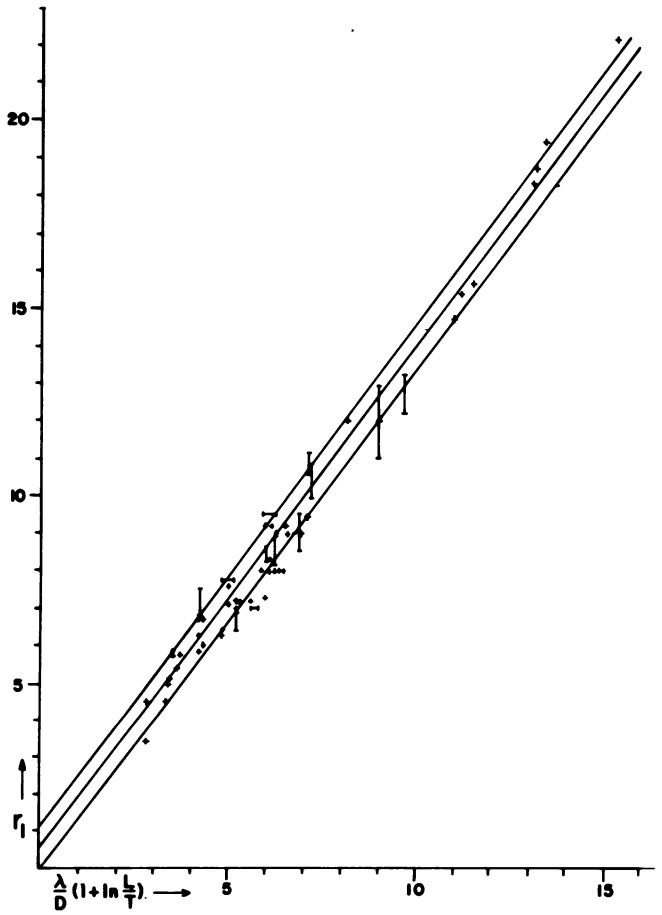

FIG. 13. Inhibitory radius (r_I) as a function of D, L, and T. Points were obtained from 60 different simulations, in some of which the inhibitory radius varied (represented by vertical lines). Fitted lines indicate the range given in formula 14.

Proof of the Completeness of the Model. In the previous section we showed simulations of (1,2,3)-, (2,3)-, and (3,5)-patterns as well as of a multijugate pattern. The question arises whether all packed circles patterns can be generated by this model. Assume that Figure 14 represents a crude picture of the concentration distribution during a simulation. The circles can be thought of as equal concentration lines of the inhibitor diffusing from a single leaf if no other leaves are present. The real concentration distribution of course is the result of a complex interaction of these circular patterns. The growth rate of the system is set so low that every leaf has enough time to reach its full inhibiting potential before the system adds another row; in other words, the system is near steady-state. At every time step there will be one cell at a minimum concentration in the whole array. Because the apex is moving upward the location of this minimum cell will shift upward too. Let us take a look at the time step in which this minimum cell is found at the same row as where the next leaf is to be generated. Let L_0 be the cell where the next leaf is to be generated and L_m and L_n the leaves closest to L_0 such that L_m is closer to the apex than L_n. If at this time L_0 is the minimum cell we can choose the threshold T just a little above its concentration so that this and only this cell is under the threshold and will turn into a leaf. If we can find the conditions under which we can be sure that this is the case, we have found the conditions under which we can be sure that every pattern can be simulated. It can be shown (*cf.* 22) that this amounts to the condition of

$$e^{-ak} + e^{-bk} > 2 \quad (15)$$

for left and right neighbors of cell L_0. Here

$$k = \sqrt{\frac{D}{2\lambda}}$$

and we denote with a the difference between the distances $L_m - L_0$ and $L_m - M$, and with b the difference between the distances $L_n - L_0$ and $L_n - M$ for both neighbors of M. If the m- and n-parastichies run in the same direction around the cylinder, a and b will have the sign, positive for one and negative for the other neighbor. It is clear that formula 15 cannot be met for both neighbors in this case and in fact a pattern like this cannot be

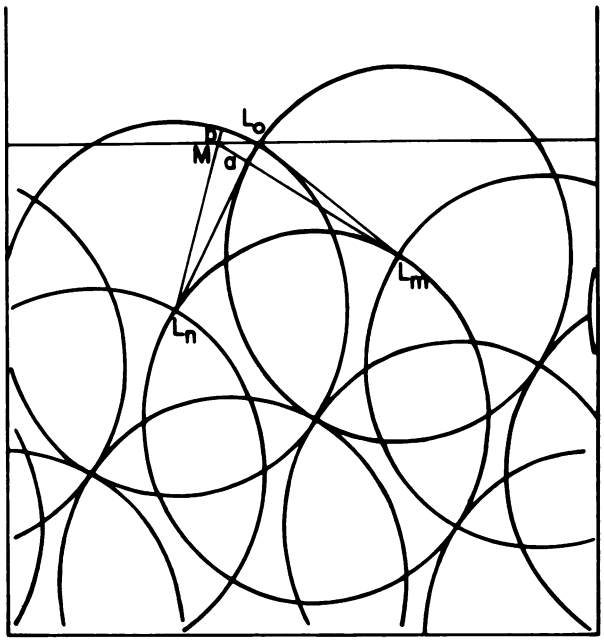

FIG. 14. Construction of intersecting circles. L is the next point of the intersecting pattern, while M is its left neighbor.

generated. The last (1,3)-pattern of Table II shows this property.

If the m- and n-parastichies run in opposite directions, it can further be shown that formula 15 certainly holds if

$$k > \frac{\ln 2}{b}$$

or (16)

$$D/\lambda > \frac{2 \ln^2 2}{b^2}$$

Since we can always find a D and λ that fulfilled this relation as well as formula 14 it has been proved that every packed circles pattern in which the m- and n-parastichies run in opposite directions can be stimulated on this model. Formulas 14 and 15 or 16 constitute a relationship between the geometric properties of a pattern and the internal parameters of the model.

The m- and n-parastichies can only run in the same direction if $n > 2m$. In fact for every $(m,n,m+n)$-triple point in Figure 3, the m- and $(m+n)$-parastichies run in one direction while the n-parastichy runs in the opposite direction around the cylinder. So of the two branches sprouting from this triple point, the $(n,m+n)$-branch always has parastichies in opposite directions while the $(m,m+n)$-branch has initially parastichies in the same direction. In Figure 7 we only drew the part of the relation for which the m- and n-parastichies run in opposite directions. So all of the patterns in this figure are in principle simulatable by the cylindrical model. It can be seen that six patterns of Table II are not part of this relationship. Although other patterns can be produced it seems that there is no other class of helical patterns that can be consistently and predictably simulated. This gives a special status to the packed circles patterns on a cylindrical surface.

We have shown that our model can generate any packed circles pattern on a cylinder if the following conditions are met. (*a*) At least $J.n$ initial leaves are placed forming a $J(m,n)$-pattern with m- and n-parastichies running in opposite directions, on an integer grid on a cylinder with a circumference of w cells with a minimum distance of $d.w$ cell units between leaves. (*b*) The values of D and λ are below and of G is above certain limits to assure a small t and an accurate computation. (*c*) The values of D and λ are such that they fulfill formula 15. (*d*) The values of D, λ, L, and T are such that substituted in formula 14 the range of r_l includes the value of $d.w$.

Relation between Physical and Simulation Parameters. The question arises whether a connection can be found between the numerical values of parameters used in the simulations and variables measured in plants. Besides the plastochron (measured in days) and the geometric properties of a phyllotactic pattern as the position of leaves and the size of a cell (in micrometers), there are biochemical factors which are in principle observable such as the diffusion constant λ^* (in m^2/sec) or permeability factor p^* (in m/sec), the decay factor D^* (per sec), the reaction time of a cell Δt (in sec) and the ratio between the highest and lowest concentration occurring within the apical region L^*/T^*. These parameters, which are superscripted with a star, are in meter-kg-sec units as opposed to our simulation parameters (written without stars) which are expressed in our own length and time units Δl and Δt. Let us look at the simulation of the (2, 3)-pattern in Figure 9b to try and draw some connections between the two sets of parameters.

The size of the cell or the length unit Δl should be about the dimension of a meristematic plant cell, that is between 10 and 50 μm. Measurements by Erickson (personal communication) on the apex of *Xanthium* show that the youngest primordium is a minimum of 50 μm away from the tip of the apex. If we take this as the radius of the cylinder we get a value of 12 μm for Δl since $w = 26$. This would correspond to about 50 cells in the apical region which is free of primordia, which seems to be a plausible number. Circumferences exceeding 50 cells would lead to improbable values.

Although the time unit Δt originally determines how accurate the diffusion calculations are, it serves also as another important factor. When the concentration of a cell drops under the threshold in a particular time step it will turn into a leaf, start producing inhibitor, and diffusing it into its surroundings within the next time step. So Δt represents the reaction time, the time it takes a cell to detect that the crucial point has been reached, to start the production mechanism—such as turning on a gene and producing the needed enzymes—and produce enough of the inhibitor to diffuse a significant amount to neighboring cells. While bacterial cells might accomplish this in 10 to 15 min, a plant cell would need at least 1 hr. The (2,3)-simulation worked well as long as G was less than 45. If the growth was faster, multiple leaves occurred which could conceivably happen in a real plant if the reaction time was not fast enough to keep up with the development of the system. A value of 45 for G means that a new leaf is produced every 90 time steps. Taking Δt as 1 hr, this would correspond to a minimum plastochron of about 4 days, a reasonable value for many plants.

The above argument holds for the chosen value of λ of 0.055. If we decrease λ (and D to keep D/λ constant) the growth has to slow down and the plastochron has to increase to allow for the leaves to get fully settled before the next leaf is initiated. There is a maximum plastochron that would still be acceptable as reasonable and it is safe to assume that values for λ under 0.01 are not realistic. The simulation has also shown that a diffusion constant higher than 0.1 gives multiple leaves. So λ should be of the order of 0.05. Thus we have for Δt and Δl estimates well within an order of magnitude. Using these and formula 7 we arrive at

$$\lambda^* = 2 \times 0.05\,(12\ \mu\text{m})^2/3{,}600\ \text{sec} = 0.4 \times 10^{-14}\text{m}^2/\text{sec}$$

within an order of magnitude. For water this would be an exceedingly small value for a diffusion constant and even the largest proteins have higher diffusion constants than this. But λ^* is the over-all diffusion constant, the average of the diffusion velocity within the cell and through the cell membrane.

There is also a maximum for the decay constant D independently of λ or G, for it is clear that D should always be less than 1. The actual maximum is probably as low as 50% decay per time step. Using formula 8 a conservative estimate is

$$D^* < 2 \times 10^{-4}/\text{sec}$$

Formula 15 gives for this pattern

$$D_{\min} > \lambda_{\min} \text{ or } D^*_{\min} > 2/\lambda^*_{\min}$$

Using the above established limits for λ we get $D > 2\%$ or $D^* > 5 \times 10^{-6}$/sec. As said before simulation is possible if D is lower than this limit but complications might arise.

Conclusions. We have given an example of how simulation parameters in our model can be translated into physical parameters. We gave order of magnitude estimates for the permeability constant and the decay rate. Although these values do not give a direct indication of what chemicals might be involved they might provide some clue as to which chemical processes might be possible. We also obtained values for the plastochron interval, the dimension of cells, and the number of cells in the apical region. For the analyzed pattern these turned out to be realistic values while for other simulations this might not be the case which would be good reason to discard them.

The strict cellularity of this model brings with it a built-in stabilization property. Deviations from the helical pattern have to be at least one cell off before they can have any effect. Smaller deviations are automatically compensated for by the fact that leaves always have integer coordinates. Every biological control system seems to need some form of feedback or self-regulation

to absorb the random fluctuations and limited precision occurring in nature, but in future refinements of the model stability should be achieved in a more realistic manner.

Another important limitation of our model is that it is based on diffusion processes taking place on cylinder surfaces. Many apices are not even approximately cylindrical, in which case other types of projections (planar or conical) may be more appropriate. One such attempt is described in reference 22. Diffusion may also take place through the core of the apex rather than on its surface only (as evoked *e.g.* by Schwabe [17]). Clearly, extended computer work should be undertaken in these directions.

Maybe the most significant aspect of this model is the fact that a rather great number of variables can be easily reduced to one parameter, the inhibiting radius r_I. This is because, generally speaking, all of the variables have either no influence on the configuration of the final pattern or only through its influence on r_I. In this way the whole variety of packed circles patterns can be simulated (or produced by a plant) by merely changing one of the variables D, λ, L, or T (or the size of the apex).

This result can also serve to take away the mystery surrounding the prominent place which Fibonacci numbers and angles play in phyllotaxis. So far our simulations have mainly been concerned with the question as to how plants maintain their phyllotactic patterns. We have shown that our mechanism can reproduce the helical pattern of inserted leaves. Just as important is the question as to how the helical patterns get established in the young plant. Imagine a very young plant having only two leaves or cotyledons in a so-called alternate or (1,1)-pattern. Imagine that the apex of the seedling increases in size but that all of the other internal factors determining its phyllotaxis remain constant. The value of d will decrease to a point where the plant has to go into a (1,2)-spiral. Depending on natural fluctuations the spiral will have equal chances to be left or right handed. Van Iterson has already shown that if on the circles on the cylinder a "constant force" should be applied directed toward the bottom of the cylinder and the cylinder was increased in size, an (m, n)-pattern would transform into an $(m, n, m + n)$-triple point and subsequently into an $(n, m + n)$-pattern rather than the $(m, m + n)$-pattern. This constant force is provided in our model by the inhibition from the tip of the apex. So by further increase in apex size a (1,2)-spiral will develop into (2,3)-, (3,5)-, or higher order Fibonacci patterns rather than into any of the other packed circles patterns. In Figure 7, this corresponds to starting at the (1,1)-line and gradually descending into any of the other line sections by decreasing d without going over "impossible" patterns indicated by gaps in the lines. If the apex increases fast enough in size the intermediate spirals would be hard to detect and only the original cotyledons and the final pattern would be observed. (A recent paper by G. M. Mitchison [13] agrees with these conclusions.)

The fact that structures as complex and as varied as plant phyllotactic patterns can be generated by a rather simple model gives us hope that the actual mechanism which controls leaf positions may also turn out to be a simple one.

ADDED NOTE

After the completion of this paper a recent article of Thornley (20) came to our attention, which seems closely related to our subject. Both his and our models are based on the diffusion of a morphogen that is produced in the primordia, decays proportionally with its concentration, and inhibits the development of a primordium as long as its concentration is above a certain threshold. Thornley avoids the problem of making assumptions about the apical shape and the influence of the tip of the apex by assuming that initiation can take place at only one circular "zone" of the apex. He studies the concentration distribution in this ring by, in effect, simulating the influence of older primordia with point sources situated at their projections on the ring. The differences in effect that the primordia have due to differences in age, size, vertical, and radial distances from the apex are all expressed in his single parameter λ which is the ratio of the strength of successive point sources. Since he further assumes that the system reaches an equilibrium in between the initiations of successive primordia he can use the analytical solutions to the one-dimensional steady-state problem (our formula 15). Rather than assuming a fixed threshold, he positions the next primordium at the lowest minimum. To facilitate the comparison between these two models we can say that Thornley's parameters α, k, D, M, β, and x_m are more or less equivalent to our $\sqrt{D/\lambda}$, D, λ, c, α, and w. His parameter λ does not correspond to any of our parameters and it is not interpretable morphologically or physiologically. It is our feeling that leaf determination is basically a two- or three-dimensional process and that one-dimensional projections of the morphogenetic field will not be sufficient to illuminate the details of its operation. We do not share Thornley's opinion concerning the prevalence of observed divergence angles close to the Fibonacci angle.

Acknowledgments—The model described in this paper was studied by us from 1969 through 1970 at the University of Utrecht. A similar model for a flat apex was studied from 1971 through 1972 at the University of Pennsylvania in Philadelphia by A. H. Veen and R. O. Erickson. The latter also supervised Veen's master thesis which describes and compares both models. Both authors acknowledge gratefully their debt to Professor Erickson for extensive discussions, sharing with us many of his stimulating ideas concerning phyllotaxis.

LITERATURE CITED

1. Adler I 1974 A model of contact pressure in phyllotaxis. J Theor Biol 45: 1-79
2. Crank J 1975 The Mathematics of Diffusion. Oxford Univ. Press, Oxford
3. Erickson RO 1973 Tubular packing of spheres in biological fine structure. Science 181: 705-716
4. Gomez-Campo C 1974 Phyllotactic patterns in *Bryophyllum tubiflorum* Harv. Bot Gaz 135: 49-58
5. Hellendoorn PH, A Lindenmayer 1974 Phyllotaxis in *Bryophyllum tubiflorum*: morphogenetic studies and computer simulations. Acta Bot Néerl 23(4): 473-492
6. Herman GT, G Rozenberg 1975 Developmental Systems and Languages. North Holland Publ Co, Amsterdam
7. Lindenmayer A 1968 Mathematical models for cellular interactions in development. Parts I and II. J Theor Biol 18: 280-315
8. Lindenmayer A 1971 Developmental systems without cellular interactions: their languages and grammars. J Theor Biol 30: 455-484
9. Lindenmayer A 1975 Developmental algorithms for multicellular organisms: a survey of *L*-systems. J Theor Biol 54: 3-22
10. Lindenmayer A, G Rozenberg, eds, 1976 Automata, Languages, Development. North Holland Publ Co, Amsterdam 529 pp
11. Maksymowych R, RE Cordero, RO Erickson 1976 Long-term developmental changes in *Xanthium* induced by gibberellic acid. Am J Bot 63: 1047-1053
12. Maksymowych R, RO Erickson 1977 Phyllotactic change induced by gibberellic acid in *Xanthium* shoot apices. Am J Bot 64: 33-44.
13. Mitchison GM 1977 Phyllotaxis and the Fibonacci series. Science 196: 270-275
14. Plantefol L 1946 Fondements d'une theorie phyllotaxique nouvelle. Ann Sc Nat Bot Serie 11 t7: 153
15. Richards FJ, WW Schwabe 1969 Phyllotaxis: a problem of growth and form. *In* FC Steward, ed, Plant Physiology, A Treatise Vol A. Academic Press, New York pp 79-116
16. Schoute TC 1913 Beiträge zur Blattstellungslehre. Rec Trav Bot Néerl 10: 153-324
17. Schwabe WW 1971 Chemical modification of phyllotaxis and its implications. *In* DD Davies, M Balls, eds, Control Mechanisms of Growth and Differentiation. Cambridge Univ Press, pp 301-344
18. Schwendener S. 1878 Mechanische Theorie der Blättstellungen. Wilhelm Engelman, Leipzig
19. Snow M, R Snow 1962 A theory of the regulation of phyllotaxis based on *Lupinus albus*. Philos Trans R Soc Lond Ser B 244: 483-513
20. Thornley JHM 1975 Phyllotaxis. I. A mechanistic model. Ann Bot 39: 491-507
21. Van Iterson G 1907 Mathematische und mikroskopisch-anatomische Studien über Blättstellungen. Gustav Fischer, Jena
22. Veen AH 1973 A computer model for phyllotaxis, a network of automata. MS thesis. Moore School, Univ Pennsylvania, Philadelphia
23. Williams RF 1974 The Shoot Apex and Leaf Growth. Cambridge Univ Press